Design of a Novel 3D Circular Vivaldi Antennas Array for Ultra-Wideband Near-Field Radar Imaging

K. Alkhalifeh[#1], R. Sarkis[#2], C. Craeye[*3]
#* Université catholique de Louvain
ICTEAM Institute, Place du Levant, 2, 1348 Louvain-la-Neuve
[1]khaldoun.alkhalifeh@student.uclouvain.be, [2]remi.sarkis@uclouvain.be, [3]christophe.craeye@uclouvain.be

***Abstract*— The design of a circular Vivaldi antenna array for Ultra wideband near-field radar imaging is presented. We first show a 3D single Vivaldi antenna with a 12:1 bandwidth without the need for complex microstrip transitions. A 3D circular array of 10 electrically connected elements is simulated using the Method of Moments, with 12:1 bandwidth. The 3D circular array is simulated using the Array Scanning Method (ASM) applied to the Method of Moments, where the ASM appears as a computationally efficient approach for simulating large circular antenna arrays. Near fields in E and H planes in the area of radiation exposure are depicted and exhibit smooth spreading over the whole field of view.**

I. Introduction

Ultra-wideband radar imaging systems involving arrays have a great interest in various short-range applications, such as medical imaging [1], through-wall observation and airport security. Large fractional bandwidth and small dimensions are critical challenges in the design of such arrays. Large bandwidth is very important for well-controlled pulse generation and high resolution. Recent studies give great interest to lower frequencies, which becomes a challenge for antenna miniaturization. Also, high resolution can be obtained by using high frequencies. The UWB technique is widely exploited in the field of medical imaging, due to the constraints of sufficient human body penetration and image resolution [2].

A uniform circular array can provide 360º azimuthal coverage and estimate source elevation angle (outside the plane of the array). In view of the cyclical symmetry of the array, the embedded element patterns are identical [3].

The proposed novel 3D circular array with large bandwidth (including lower frequencies) presents the following advantages for medical imaging applications: low cost fabrication, low power, no mechanical complications (scanning or switching) and fast data acquisition (which provides a comfort for the patient and helps to get accurate tumor locations [4]) .

This paper is organized as follows: the design of a compact 3D Vivaldi antenna is provided in section II. Section III presents the 3D circular Vivaldi antenna array structure, as well as simulation results. Section IV provides simulation results for the array using the Array Scanning Method. The homogeneity of UWB near fields (wide field of view) is illustrated in section V. Conclusions are drawn in Section VI.

II. Design of Isolated 3D Vivaldi Antenna

The proposed design, shown in Fig. 1, has the following dimensions:

- Width a=10 cm, length b=9 cm.
- Circular cavity of diameter d=1.1 cm.
- Feed region: 0.2 cm by 0.2 cm.
- Thickness of 0.5 cm.
- Type of taper profile: elliptical.

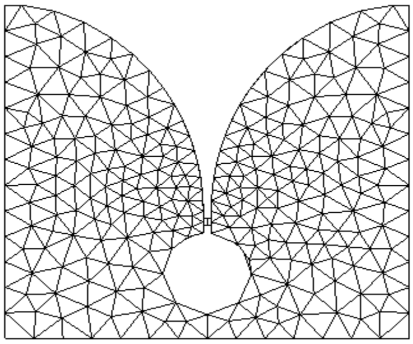

Figure 1. Layout of the 3D Vivaldi antenna

This antenna is designed and meshed using GMSH [5]. A software developed at UCL based on the Method of Moments (MoM3D) code is used to simulate the different structures. Fig. 2 shows the simulated reflection coefficient of the single Vivaldi antenna with reference to 50 Ω.

For the presented antenna, the simulation result exhibits a bandwidth from 2.34 GHz to 14 GHz with respect to a -10 dB criterion for the antenna reflection coefficient. Meanwhile, if we consider that -5 dB for the antenna reflection coefficient is sufficient near the lowest frequency (large penetration); we have a lower frequency of 0.83 GHz.

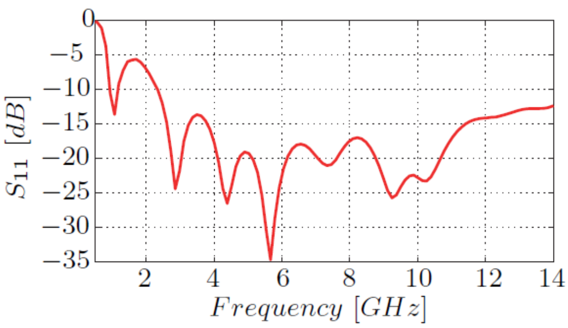

Figure 2. Reflection coefficient bandwidth of the single antenna

III. 3D CIRCULAR VIVALDI ANTENNAS ARRAY (3DCA)

Ten Vivaldi antennas are arranged in a circular array with length of 32.4 cm and width of 30.7 cm and an inner diameter of 15.2 cm (Fig. 3).

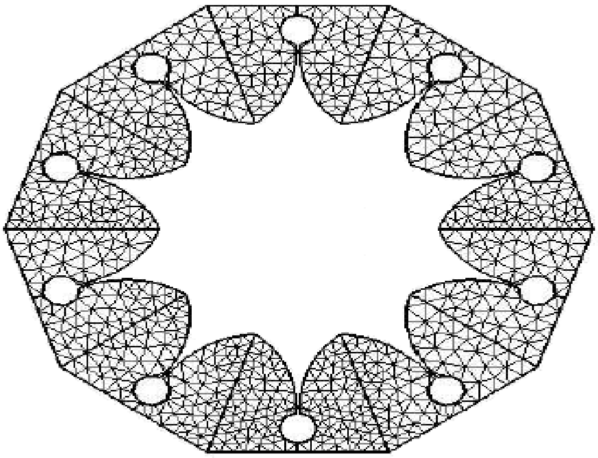

Figure 3. 3D Circular Vivaldi array layout.

We consider the case of excitation at one port in the circular array, while the remaining antennas are passively terminated.

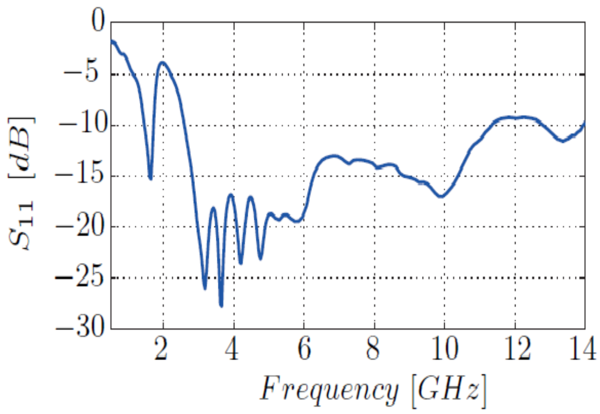

Figure 4. Reflection coefficient bandwidth of the connected circular array.

Fig. 4 shows the reflection coefficient bandwidth for connected elements case (we connect elements using overlapping triangular basis functions); good results can be achieved in terms of matching of the elements. We notice a satisfactory bandwidth for the reflection coefficient under -10 dB from 2.5 to 14 GHz. In the same way, as previously, we can obtain 1.1 GHz as a lower frequency if we consider that -5 dB for the antenna reflection coefficient is sufficient near the lowest frequency (large penetration).

IV. RESULTS BASED ON ASM

The array Scanning Method (ASM) [6] was applied in [7], for the accurate solution of finite-by-infinite arrays excited at a single port. In the case of a circular array of N elements excited at one port, while the remaining antennas are passively terminated, the currents can be obtained by using the phase mode excitations [8], with the help of the ASM [9]. The current excited at antenna m for antenna 0 active appears as:

$$I(m)=\frac{1}{N}\sum_{p=0}^{N-1} I^{\infty}(\psi_p)e^{-jm\psi_p}$$

Where $I^{\infty}(\psi)$ is the current distribution when all the N elements are excited. Ψ is the phase shift between elements, and it is equal to $\psi_p = p\frac{2\pi}{N}$ $(0 < p < N\text{-}1)$.

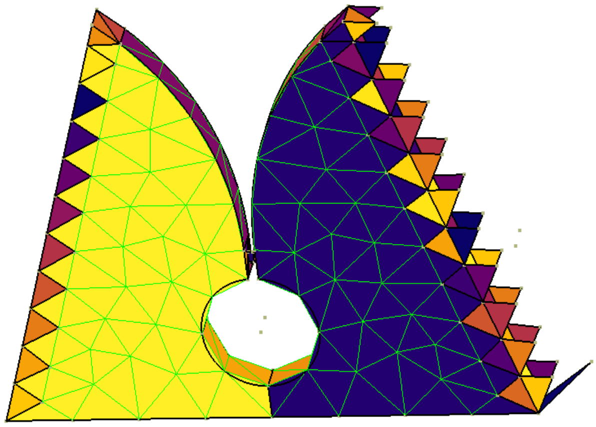

Figure 5. Meshed single Vivaldi antenna with connecting basis functions.

Overlapping basis functions are used to ensure the flow of current between successive elements (Fig. 5), and to get the exact results (within limits implied by discretization).

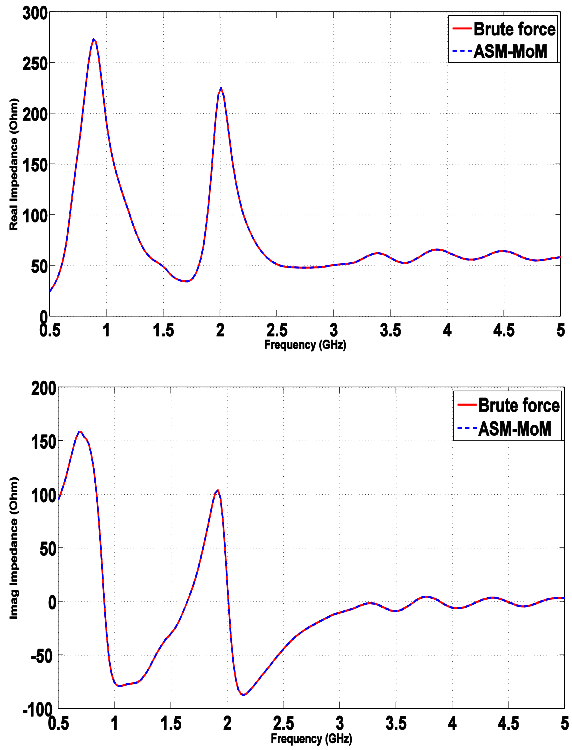

Figure 6. Real (a) and imaginary (b) impedance parts comparison between MoM3D and ASM-MoM methods.

We observe in Fig. 6 that the results obtained by applying the ASM-MoM and brute force methods are practically identical. The ASM method helps us to reduce the computation time without affecting the accuracy of the input impedance. Computation times for 80 frequency points are given in table I.

TABLE I. ELAPSED SIMULATION TIME COMPARISON

Brute force-MoM elapsed simulation time	16 hours
ASM-MoM elapsed simulation time	1 hour 36 min

V. UWB NEAR-FIELD RADIATION OF THE 3DCA

A microwave holography method [10] is applied to study the signal interference between the fields radiated by an antenna under test (AUT) and those scattered by a near-field target. Measurement of the amplitude and the phase of the near field radiated by the AUT is a common way to evaluate the potential sensitivity of the system. A brief introduction to the mutual coupling phenomenon is presented. Then, the current distribution over all the antenna elements with a study of the near-field in the middle of 3DCA is depicted.

A. Mutual coupling study

Mutual coupling is a common problem in various antenna arrays, and it impacts all types of antenna array parameters, such as the input impedance and the radiation pattern. In other words, the input impedance of a single element in an array differs from that of the same element when it is isolated, due to the mutual coupling effect [11].

To distinguish the mutual coupling effect, a comparison is made between the isolated Vivaldi antenna (Fig. 7.a) and by putting it in the array (Fig. 7.b).

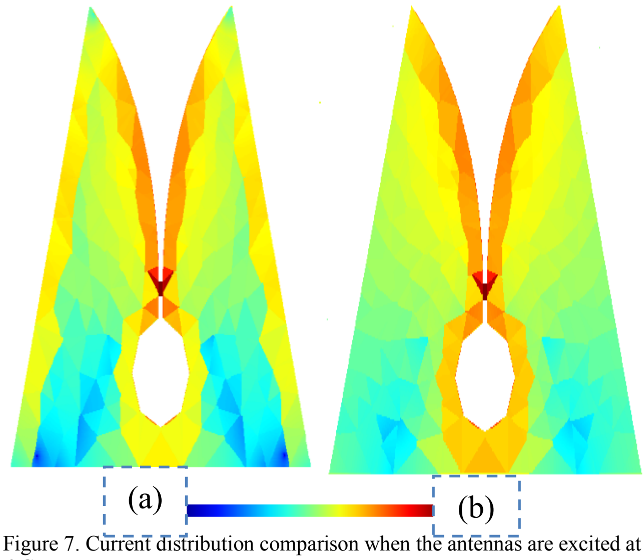

Figure 7. Current distribution comparison when the antennas are excited at 6 GHz.

Fig. 7.b shows the appearance of higher current distribution regions compared with that of Fig. 7.a on the antenna body and near the circular cavity, which reflects an exchange of the current between the original source and its neighbors. Fig. 7 also shows that the highest radiation of the antennas comes from a small section along the curve of the flare. Also, edge currents disappeared in the connected structure.

B. UWB Near-field radiation study

Fig. 8 shows the current flows from the basic source to the other elements, where the source's neighbors are the most affected. The third and sixth elements (we count the source as the antenna 0) are less affected, probably through a combination of distance and polarization mismatch.

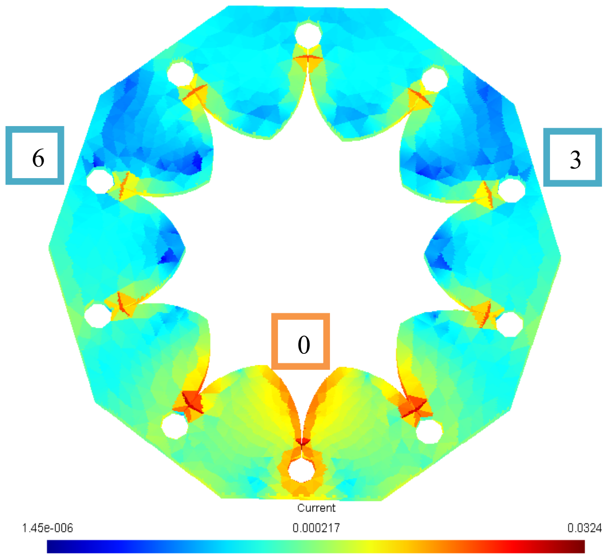

Figure 8. Current distribution on the 3D circular antennas array

To know more about the near-field sensitivity, a 2D rectangular screen of testing functions is created in the UWB near-field exposure region. A function has been developed to generate the testing functions and to draw the geometrical position of the 2D screen and the antennas array (Fig. 9). The dimensions of the 2D screen are 6.8 cm by 6.2 cm.

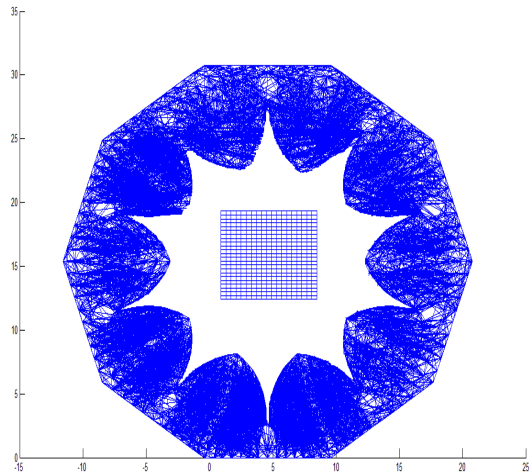

Figure 9. The geometrical position of the antennas array and the 2D screen.

The radiated field can be obtained from the following equation, by taking into account the mutual coupling between the antennas in the array:

$$\underline{E} = \underline{\underline{Z}}_{AR} . \underline{I}$$

This also expresses to the near-field sensitivity, where $\underline{\underline{Z}}_{AR}$ is the MoM impedance matrix obtained between the 3DCA and the 2D screen. $\underline{I}$ is the current distribution on the antenna when it is excited in the array. The testing functions are oriented according to the polarization of the antennas in E-plane (Fig. 10.a), and then in H-plane (Fig. 10.b).

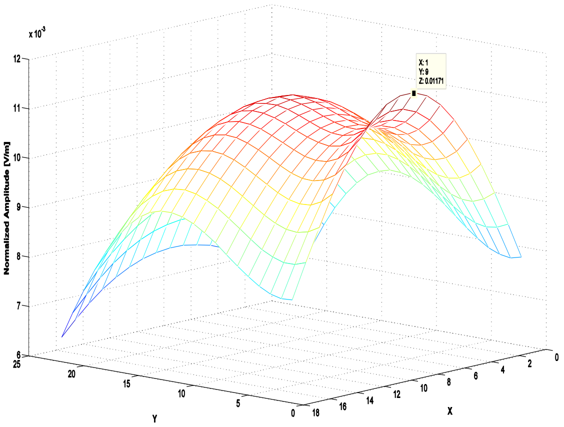

(a)

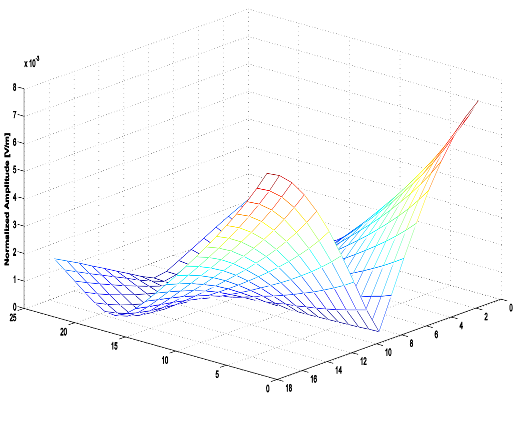

(b)

Figure 10. Normalized amplitude (V/m) of the equivalent field distributions of the 3DCA in (a) E-plane and (b) H-plane, for one antenna excited.

Fig. 10 depicts near-field radiation for UWB array of 10 elements excited at one element in E and H planes. X and Y indices (a grid of 18×22 lines) refer to the 2D screen testing function points. Fig. 10.a shows a larger field of view along the X axis than along the Y axis. The lower near-field radiation is located in the two far 2D screen corners from the source; this is consistent with lower excitation of antennas 3 and 6 (Fig. 8), as mentioned in section V. B. A smooth near field shape in the middle of the antenna array is observed at 2 GHz.

In Fig. 10.b, a line can be seen exactly in the middle of X axis, where the cross-pol is low. This line corresponds to the plane of symmetry of the structure that crosses the feed points. Also, despite the mutual coupling, the near-field radiation of a given antenna remains perfectly symmetrical.

VI. CONCLUSION

We present the design and simulation of a 3D circular array of Vivaldi antennas for UWB near-field imaging. The 3D circular array with dimensions 32.36 cm by 30.7 cm and an inner diameter of 15.2 cm achieves satisfactory radiation performance over the bandwidth from 2.5 GHz to 14 GHz with 140% fractional bandwidth. A fast calculation method has been proposed for circular arrays devoted to near-field imaging. The mutual coupling phenomenon is briefly discussed. A relatively homogenous (< 6 dB variation) response has been obtained over the whole field of view, which is a necessary condition for near-field imaging based on delay-and-sum or interferometric methods.

REFERENCES

[1] M. Klemm, J. Leendertz, D. Gibbins, I. Craddock, A. Preece, and R. Benjamin, "Microwave radar-based differential breast cancer imaging: imaging in homogeneous breast phantoms and low contrast scenarios," IEEE Trans. Ant. Prop., vol. 58, pp. 2337 – 2344, July 2010.

[2] Al-Joumayly, M.A.; Aguilar, S.M.; Behdad, N.; Hagness, S.C., "Dual-band miniaturized patch antennas for microwave breast imaging," IEEE Trans. Antennas and Wireless Propagation Letters, vol. 9, pp.268-271, 2010.

[3] C. M. Tan, P. Fletcher, M. A. Beach, A. R. Nix, M. Landmann, and R. S. Thomä, "On the application of circular arrays in direction finding part I: investigation into the estimation algorithms," 1st Annual COST 273 Workshop, Finland, May 2002.

[4] M. Bialkowski and Y. Wang, "UWB cylindrical microwave imaging system employing virtual array antenna concept for background effect removal," Microwave and Optical Technology Letters, vol. 53, pp. 1100-1104, May 2011.

[5] GMSH, a three-dimensional finite element mesh generator with built-in pre- and post-processing facilities. http://www.geuz.org/gmsh/.

[6] B.A. Munk and G.A. Burrell, "Plane-wave expansion for arrays of arbitrarily oriented piecewise linear elements and its application in determining the impedance of a single linear antenna in a lossy halfspace," IEEE Transl. Ant. Prop., vol. 27, no. 5, pp. 331–343, May 1979.

[7] C. Craeye and R. Sarkis, "Finite array analysis through combination of macro basis functions and array scanning methods," Journal of the Applied Computational Electromagnetics Society, vol. 23, 256-261, 2008.

[8] C. P. Matthews and M. D. Zoltowski, "Eigenstructure techniques for 2-D angle estimation with uniform circular arrays," IEEE Transactions on Signal Processing 42, pp. 2395–2407, 1994.

[9] R. Sarkis, C. Craeye, "Circular array of wideband 3D Vivaldi antennas," Electromagnetic Theory (TMTS), Berlin, Germany, 16-19 Aug. 2010.

[10]G. Junkin, T. Huang, J.C. Bennett , "Holographic near-field/far-field for terahertz antenna testing", IEEE Trans. Ant. Prop., vol. 48, no. 3, pp 409-417, March 2000.

[11] C. Craeye, D. González-Ovejero. "A review on array mutual coupling analysis," Radio Science - RADIO SCI, vol. 46, no. RS2012, pp. 25, 8 April 2011.